American College of Neuropsychopharmacology

www.nature.com/npp

ARTICLE

Check for updates

Selective KOR antagonist alters functional patch sizes in individualized brain system: results from the Fast-fail Trial in Mood and Anxiety Spectrum Disorders (FAST-MAS)

Hoki Fung[1], Ruby M. Potash[1], Andrew Krystal[2], Diego A. Pizzagalli[3,4,5] and Matthew D. Sacchet[1]✉

In our prior study involving a transdiagnostic sample of individuals with anhedonia, we showed that an 8-week administration of a selective κ-opioid receptor (KOR) antagonist enhanced fMRI ventral striatal activation during reward anticipation in the Monetary Incentive Delay task as compared to a placebo. However, individual differences in brain architecture may limit the translation of this finding to the context of precision medicine. Here, we adopted an individual-specific approach to elucidate the effects of selective KOR antagonism on cortical-subcortical reward circuits in individuals with anhedonia. Sixty-four participants with anhedonia (30 KOR Antagonist, 34 Placebo) who completed both pre- and post- treatment MRI scans in the FAST-MAS study were included in this analysis. Using an individualized-brain-systems-functional-brain-mapping approach, functional networks were mapped at the individual level, and individual-specific cortical patches and subcortical-cortical clusters were obtained. Statistical analyses were conducted to examine the pre- and post-treatment changes in patch and cluster sizes, as well as their relationships with clinical-cognitive measures. ROI analyses revealed a significant patch size decrease in the right medial posterior prefrontal cortex within the frontoparietal control network, and significant size increases in three right subcortical clusters – pallidum, amygdala, and thalamus – within the orbitofrontal-limbic network, following KOR antagonist treatment. In short, we applied recently developed computational neuroimaging approaches to examine changes in the individualized brain systems of FAST-MAS participants before and after eight weeks of KOR antagonist treatment for anhedonia. Our results revealed alterations in functional cortical patch and subcortical-cortical cluster sizes in anhedonia-related brain regions following KOR antagonist treatment.

Neuropsychopharmacology; https://doi.org/10.1038/s41386-025-02125-z

INTRODUCTION

Anhedonia, characterized by a reduced ability to experience pleasure, is a core feature in mood and anxiety disorders [1], including Major Depressive Disorder (MDD), affecting approximately 70% of MDD patients [2]. It is also a common symptom in various psychiatric conditions such as schizophrenia, substance use disorders, and post-traumatic stress disorder [3]. Across diagnoses, unmanaged anhedonia is associated with a less favorable prognosis and an elevated risk of suicidal behavior [4]. Conversely, the amelioration of anhedonia is correlated with better quality of life in individuals with mood disorders [5] and improved psychosocial functioning in MDD patients [6]. In addition, anhedonia severity is associated with illness severity [7, 8], striatal volume [9], and neural activities in various brain regions [10, 11]. It has also been found to mediate the relationship between neural reward responsiveness and quality of life in mood disorders [5]. Given its relevance across psychiatric disorders, anhedonia warrants consideration as a transdiagnostic treatment target [12], aligning with the dimensional approach to psychopathology outlined in the National Institute of Mental Health's Research Domain Criteria (RDoC) framework [13, 14]. However, typical first-line treatments for mood and anxiety disorders like antidepressant selective serotonin reuptake inhibitors (SSRIs) and serotonin norepinephrine reuptake inhibitors (SNRIs), show limited effectiveness in ameliorating anhedonia [3]. This has prompted several recent clinical trials focused on uncovering effective interventions and treatments for anhedonia [12, 15], such as the Fast-fail Trial in Mood and Anxiety Spectrum Disorders (FAST-MAS) study (ClinicalTrials.gov Identifier: NCT02218736).

The FAST-MAS study is a multi-center, eight-week, double-blind, randomized placebo-controlled trial to evaluate the efficacy of a selective κ-opioid receptor (KOR) antagonist as a potential treatment for anhedonia in mood or anxiety disorders [4, 15]. KOR antagonists are emerging as promising treatments for a wide range of psychiatric conditions, including depression, anxiety, and substance abuse [16]. Preclinical research investigating stress paradigms in animal models has established the general ability of KOR antagonists to mitigate the effects of stress, a common trigger and exacerbator of these conditions, through various molecular mechanisms (for a review, see ref. [16]). In addition to

[1]Meditation Research Program, Department of Psychiatry, Massachusetts General Hospital, Harvard Medical School, Boston, MA 02129, USA. [2]Department of Psychiatry and Behavioral Sciences, University of California San Francisco, San Francisco, CA 94143, USA. [3]Department of Psychiatry, Harvard Medical School, Boston, MA 02114, USA. [4]Center for Depression, Anxiety and Stress Research, McLean Hospital, Belmont, MA 02478, USA. [5]McLean Imaging Center, McLean Hospital, Belmont, MA 02478, USA.
✉email: meditationadministration@mgh.harvard.edu

Received: 24 March 2025 Revised: 16 April 2025 Accepted: 1 May 2025
Published online: 13 May 2025

stress regulation, KOR antagonists have demonstrated the capacity to modulate reward-related function and prevent the development of anhedonic-like states by normalizing the mesolimbic dopamine system [15, 17]. Specifically, KOR agonists decrease nucleus accumbens dopamine release and increase anhedonia-like behavior, while KOR antagonists produce the opposite effect [15]. Although human studies are limited, the initial examinations of the FAST-MAS data, focusing on ventral striatum activation during reward anticipation [15] and performance in reward learning tasks [4], have yielded encouraging results. The anticipation of reward is closely related to the experience of pleasure, as impairments in reward anticipation often co-occur with diminished pleasure from actual rewards, particularly in the context of anhedonia [18]. In the study, a transdiagnostic sample of individuals with anhedonia (Snaith-Hamilton Pleasure Scale [SHAPS] score ≥20), an 8-week administration of a selective KOR antagonist led to positive changes in clinical outcomes (i.e., lower baseline-adjusted mean SHAPS score), improved behavioral performance (i.e., higher learning rate in the Probabilistic Reward Task [PRT]), and enhanced neural responses (i.e., greater mean ventral striatal activation during reward anticipation in the Monetary Incentive Delay [MID] functional Magnetic Resonance Imaging [fMRI] task) in comparison to a placebo. These findings have illuminated the potential for KOR antagonists to address anhedonia in a transdiagnostic population, but further research is needed to establish their clinical viability, including a deeper understanding of underlying neural mechanisms and their effectiveness across individuals.

In the present study, we used an individualized brain systems mapping approach to investigate neural mechanisms by which a selective KOR antagonist affects cortical-subcortical reward circuitry in individuals with anhedonia. We applied a recently developed iterative parcellation procedure to map cortical functional networks at the individual level [19], followed by a homologous functional region ("patch") mapping method [20] to identify discrete regions that exhibit highly correlated activity unique to the individuals ("individualized functional patches"). Furthermore, subcortical parcellation was performed using a modified winner-take-all approach [21], where each of the subcortical regions was further divided into network-specific subregions that are specific to the individuals. We then investigated the relationships among treatments, individualized patch sizes, and clinical outcomes.

Patches derived through this individualized brain systems functional brain mapping approach encapsulate spatial and functional organizational information unique to each individual. Given that the amount of brain territory allocated to a cognitive function often reflects its functional significance or capability [22], patch sizes are behaviorally relevant and can serve as a meaningful measure of the relationship between brain and behavior. For instance, Kong et al. demonstrated that the size of individual-specific cortical networks can predict behavioral measures in humans [23]. In addition, using the individualized brain systems functional brain mapping approach to examine data from the Establishing Moderators and Biosignatures of Antidepressant Response in Clinical care (EMBARC) study [24], Sacchet et al. found that MDD patients with significantly smaller patches in the lateral salience system and the control system display more cognitive deficits and heightened anxious arousal [25].

The interplay between an individual's unique brain architecture and the response to KOR antagonists remains unknown. By elucidating the relationship between individualized brain systems and the effects of KOR antagonists using the individualized brain systems functional brain mapping approach, this study seeks to contribute to the advancement of precision medicine, paving the way for more personalized, mechanistically grounded, and optimized treatments for anhedonia across various disorders.

METHODS AND MATERIALS

The FAST-MAS study

The Fast-fail Trial in Mood and Anxiety Spectrum Disorders (FAST-MAS) study is a multi-center, eight-week, double-blind, randomized placebo-controlled trial to evaluate the efficacy of KOR antagonist as a potential treatment for anhedonia in mood or anxiety disorders (ClinicalTrials.gov Identifier: NCT02218736).

Study participants

The FAST-MAS study recruited participants between the ages of 21 and 65, who at the time of recruitment, exhibited some degree of anhedonia (SHAPS score ≥20, using dimensional scoring guidelines) and met the DSM-IV-TR diagnostic criteria for a mood or anxiety disorder. The recruitment took place at six research centers across the United States, and the study protocol was approved by each local institutional review board. All participants provided informed written consent before enrollment. For a detailed account of the experimental procedure in the FAST-MAS study, refer to [15].

A total of 163 individuals enrolled in the study, 94 met the inclusion criteria, and 89 completed the baseline assessments. The 89 participants were randomly assigned to either the KOR Antagonist ($n = 45$) or Placebo ($n = 44$) groups. Participants in the KOR Antagonist group were administered a 10 mg dose of Aticaprant (developmental codes: JNJ-67953964, CERC-501, LY-2456302) daily over the eight weeks, while the Placebo group received an identical-looking placebo tablet daily over the eight weeks. Among these 89 participants, 64 (30 KOR Antagonist, 34 Placebo) completed the study with both MRI scanning sessions, and were therefore, included in the analyses presented in this paper. Table 1 summarizes the demographic and clinical-cognitive profiles of the 64 participants included in the present study.

Study design and materials

An array of clinical, cognitive, and neuroimaging measures, including the Snaith-Hamilton Pleasure Scale (SHAPS), Temporal Experience of Pleasure Scale (TEPS), Hamilton Rating Scale for Depression (HAM-D), Hamilton Rating Scale for Anxiety (HAM-A), Clinical Global Impression (CGI), Cognitive and Physical Functioning Questionnaire (CPFQ), Probabilistic Reward Task (PRT), and multimodal Magnetic Resonance Imaging (MRI) images, were collected from participants at baseline and eight weeks later in the FAST-MAS study.

The present study examined the multimodal MRI data collected in the FAST-MAS study, including high resolution T1-weighted images, resting-state fMRI, and task-based fMRI, to investigate putative changes in individualized brain systems before and after eight weeks of double-blind treatment. The study also explored the associations between these neurological changes and changes in clinical-cognitive outcomes.

Figure 1 illustrates an overview of study design and analysis approaches. For a detailed description of the study participants and measures utilized in the present study, as well as information on the MRI acquisition and preprocessing procedures, please refer to the supplementary materials.

Primary outcomes

Individualized brain systems: cortical patch sizes. An individual-level cortical parcellation approach [19, 20] was used to map the functional architecture and extract cortical region sizes, that is, cortical patch sizes, at the individual subject level.

First, a population-level functional atlas which consists of 116 regions in 17 cortical networks [26] was projected onto the subjects' structural scans. Each subject's resting-state and MID task-based fMRI runs were concatenated into a continuous run, similar to other individualized brain system mapping approaches [19–21, 25]. With the initial group-level parcellation, the average time courses of the blood-oxygen-level-dependent (BOLD) signals from the individual subject's concatenated task and resting-state fMRI scans were computed for each network. In other words, for each participant, we derived a set of 17 atlas-based network time courses by averaging the BOLD time courses across all vertices within each network as defined by the population-level atlas. These time courses served as the reference signals for the optimization procedures that followed.

Next, an iterative search process making use of these reference signals and several weighting parameters was applied to refine the vertex assignments, so that the final parcellation integrates the unique functional architecture within each individual. A full description of the iterative

process and parameters involved can be found in ref. [19]. Essentially, the functional MRI signal at each vertex in different networks was compared to the reference signals from the 17 networks and then (re)assigned to the network that gave the strongest correlation, indicating a robust alignment with the distinctive activity patterns characterizing that network. A confidence value was also calculated for each vertex by dividing the largest correlation value with the second-largest correlation value. If this value was greater than a predefined threshold (1.1, as chosen for this study, which according to wang et al. [19] indicates high confidence in the network membership of vertices), the vertex would be considered a core component of the assigned network and included in the subsequent computation of the weighting parameters. The resulting signal estimate was a weighted signal of the original reference signals and the core signal (average of signals from the core vertices), and used as the new reference signal for the next iteration. This process was iterated until network membership remained the same for 98% of the vertices in two consecutive iterations.

Once the individualized cortical networks were obtained, the networks were segmented into discrete "patches" using a clustering algorithm provided in the Connectome Workbench (https://www.humanconnectome.org/software/connectome-workbench). These patches were then matched, network-by-network, to the 116 cortical regions as defined by the reference population-level atlas. The matching was done based on the number of overlapping vertices (≥20) and nearest-neighbors in cases where there were no overlaps. For more details, see ref. [20]. Finally, the cortical patch sizes were defined as the number of vertices within the individualized regions.

Individualized brain systems: cortical-subcortical cluster sizes. To obtain the individualized cortical-subcortical cluster sizes, we first segmented 14 subcortical structures (bilateral amygdala, hippocampus, thalamus, caudate, nucleus accumbens, putamen, and pallidum) using FreeSurfer (https://surfer.nmr.mgh.harvard.edu). We then extracted the average BOLD time courses from each of the 17 cortical networks in the individualized brain systems. Next, we mapped the individualized cortical systems to the subcortex (to identify the representation of that system in the subcortex). Pearson correlations between each subcortical voxel and each of the individualized cortical networks were calculated [21, 27]. Fisher's r-to-z transform was then applied to normalize the correlation values across the subjects. With the correlation values, each voxel in the 14 subcortical regions was assigned to the cortical system with which it positively correlated with the most. Finally, the individualized cortical-subcortical cluster sizes were defined as the number of subcortical voxels in a cortical-subcortical cluster. For more details regarding this approach, refer to [21, 27].

Secondary outcomes

The summary scores from SHAPS, TEPS, HAM-D, and HAM-A, as well as the CGI-S score from CGI were used to evaluate clinical symptoms. The CPFQ score, PRT reward sensitivity, and PRT learning rate were used to assess cognitive functioning.

Statistical approach

Changes in cortical patch size and subcortical-cortical cluster size

Mixed-effects model: We investigated the relationships between treatment and patch/cluster sizes by employing a mixed-effects model using R (version 4.2.2, http://www.r-project.org). The model examined how patch/cluster size is influenced by the interaction between *Group* (placebo and KOR antagonist) and *Session* (baseline and week 8), considering factors such as age and gender, and accounting for individual differences through random effects.

Spreading interactions: One of the main objectives of the current study is to identify cortical brain regions and cortical-subcortical clusters in which the KOR antagonist group exhibited significant changes from pre- to post-treatment while the placebo group did not. To test this hypothesis, we specified a contrast that tested for pre-treatment (baseline) to post-treatment (week 8) *change* in the treatment group and *no change* in the placebo group using the following contrast weights: [−1 (placebo, pre-treatment), −1 (KOR antagonist, pre-treatment), −1 (placebo, post-treatment), 3 (KOR antagonist, post-treatment)]. This approach (as seen in refs. [28, 29]) compares the treatment group at post-treatment with the average of the other cells in the 2 (Group) x 2 (Session) design and isolates the spreading interaction pattern from other patterns such as the

Table 1. Demographic information and clinical-cognitive profiles of study participants.

Variable	Placebo ($N = 34$)[b]		KOR Antagonist ($N = 30$)[b]		Baseline[c]		Week eight[c]	
	Baseline	Week eight	Baseline	Week eight	*t*-statistic	*p*-value	*t*-statistic	*p*-value
Demographics								
Mean Age in Years (SD)	39.4 (13.4)		39.8 (14.2)					
Gender - %Female	55.9		56.7					
Clinical symptoms								
Mean SHAPS[a] (SD)	33.6 (5.22) ($N = 34$)	31.4 (6.76) ($N = 34$)*	35.9 (7.77) ($N = 30$)	31.8 (7.68) ($N = 30$)*	−1.40	0.17	−0.22	0.83
Mean TEPS[a] (SD)	55.0 (16.6) ($N = 34$)	59.8 (18.8) ($N = 34$)*	55.9 (16.7) ($N = 30$)	61.9 (15.3) ($N = 30$)*	−0.21	0.83	−0.49	0.63
Mean HAM-D[a] (SD)	15.0 (5.95) ($N = 34$)	10.9 (7.29) ($N = 34$)*	14.3 (4.73) ($N = 30$)	9.90 (6.80) ($N = 30$)*	0.57	0.57	0.59	0.56
Mean HAM-A[a] (SD)	15.6 (7.16) ($N = 34$)	10.8 (7.36) ($N = 34$)*	13.5 (4.89) ($N = 30$)	9.60 (7.39) ($N = 30$)*	1.33	0.19	0.65	0.52
Mean CGI-S[a] (SD)	3.97 (0.521) ($N = 34$)	3.21 (1.01) ($N = 34$)*	3.80 (0.484) ($N = 30$)	3.00 (1.05) ($N = 30$)*	1.36	0.18	0.80	0.43
Cognitive functioning								
Mean CPFQ[a] (SD)	24.9 (5.74) ($N = 34$)	20.1 (6.77) ($N = 34$)*	25.7 (5.91) ($N = 30$)	20.9 (6.99) ($N = 30$)*	−0.56	0.58	−0.42	0.68
Mean PRT[a] Reward Sensitivity (SD)[d]	1.13 (0.285) ($N = 28$)	1.18 (0.337) ($N = 28$)	1.10 (0.272) ($N = 23$)	1.08 (0.283) ($N = 23$)	0.34	0.73	1.23	0.22
Mean PRT[a] Learning Rate (SD)[d]	−3.62 (1.06) ($N = 28$)	−4.15 (0.864) ($N = 28$)*	−3.89 (0.878) ($N = 23$)	−3.70 (0.876) ($N = 23$)	1.00	0.32	−1.83	0.07

Descriptive summary of participant characteristics in the present study by Group (Placebo and KOR Antagonist) and Session (Baseline and Week Eight).
[a]*SHAPS* Snaith-Hamilton Pleasure Scale, *TEPS* Temporal Experience of Pleasure Scale, *HAM-D* Hamilton Rating Scale for Depression, *HAM-A* Hamilton Rating Scale for Anxiety, *CGI-S* Clinical Global Impression Scale (Severity), *CPFQ* Cognitive and Physical Functioning Questionnaire, *PRT* Probabilistic Reward Task.
[b]Paired t-tests were performed on each variable for baseline and week eight within each group. Variables showing a significant difference ($p < 0.05$) between baseline and week eight are indicated with an * at Week Eight.
[c]Two-sample t-tests were performed on each variable at Baseline and Week Eight. No significant differences were observed between the Placebo and KOR Antagonist groups.
[d]Fewer participants were included in the PRT analyses due to missing data.

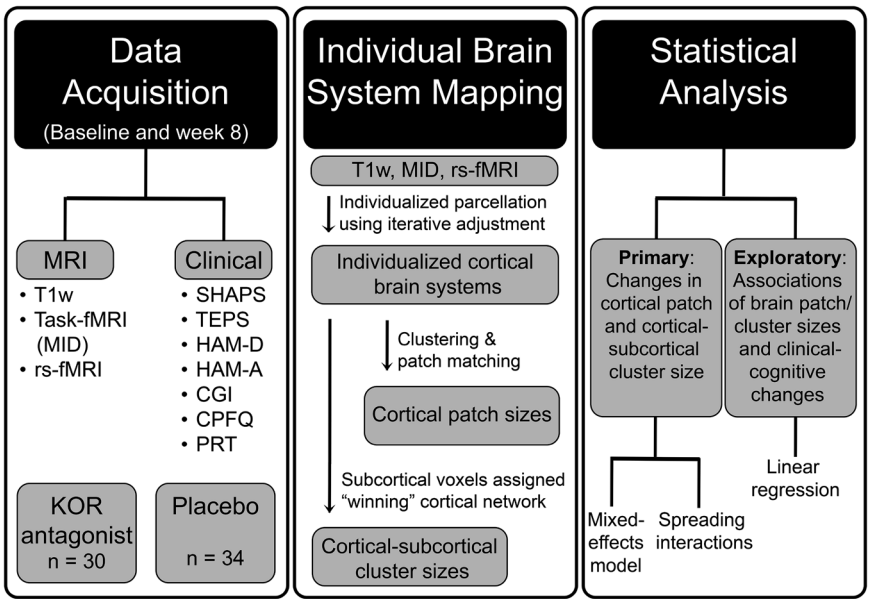

Fig. 1 Workflow of methodological pipeline. Data were acquired from the Fast-fail Trial in Mood and Anxiety Spectrum Disorders (FAST-MAS) study (ClinicalTrials.gov Identifier: NCT02218736) and included both MRI (T1-weighted images, resting-state [rs-fMRI], and monetary incentive delay [MID] task-based fMRI) and clinical-cognitive measures (SHAPS Snaith-Hamilton Pleasure Scale, TEPS Temporal Experience of Pleasure Scale, HAM-D Hamilton Rating Scale for Depression, HAM-A Hamilton Rating Scale for Anxiety, CGI-S Clinical Global Impression Scale (Severity), CPFQ Cognitive and Physical Functioning Questionnaire, PRT Probabilistic Reward Task). Individualized brain systems (17 networks [26]) were derived from T1w images and combined MID/rs-fMRI data through an iterative parcellation process and then clustered into cortical "patches" corresponding to 116 regions of the cortex [19, 20]. Patch sizes were defined as the number of vertices within the individualized regions. Average time courses of cortical networks and each subcortical voxel were correlated, assigning a "winning" network to each subcortical voxel [21]. The individualized cortical-subcortical cluster sizes were defined as the sum of subcortical voxels in a cortical-subcortical cluster. Finally, changes in cortical patch and subcortical-cortical cluster size across groups (KOR antagonist, $n = 30$; Placebo, $n = 34$) and sessions (baseline and week 8) were assessed using a mixed effect model and spreading interaction analysis. Exploratory analyses examined relationships between changes in brain patch/cluster sizes and clinical-cognitive changes using linear regression.

crossover interaction. Estimates were plotted to confirm the specific interaction pattern of interest.

Networks and regions of interest (ROIs): All analyses were first conducted at the whole-network level. In addition, drawing from existing literature and prior research findings [25], we identified a set of ROIs encompassing the medial posterior prefrontal cortex (PFCmp) in the frontoparietal control network (for more information on this ROI, please refer to refs. [26] and [30]) and 14 bilateral subcortical structures in the orbitofrontal-limbic network. The selection of these specific patches and clusters was guided by their significance in relation to reward processing in anhedonia.

Multiple comparison correction: The *p*-values from the whole-network level statistical models were corrected for multiple comparisons using the Benjamini–Hochberg procedure to control the False Discovery Rate (FDR) at 0.05 [31]. Given a priori hypotheses for the ROI analysis, the same correction was carried out separately for bilateral PFCmp, thalamus, amygdala, hippocampus, and subcortical structures in the reward circuit (caudate, nucleus accumbens, putamen, and pallidum).

Exploratory analysis

The current study only included data points from FAST-MAS participants who completed both MRI scans. While the KOR antagonist group in the current study showed improvements in anhedonia and some clinical-cognitive measures (see Table 1) – unlike the full sample as reported by Krystal et al. in 2020 [15] – these improvements were not significantly different from those observed in the placebo group (see Table 1). Hence, examining the relationship between alterations in brain patch and cluster sizes and changes in clinical-cognitive measures may not yield straightforward interpretations. Nevertheless, for the completeness of the current study, we included an exploratory analysis investigating the association between brain changes and clinical-cognitive changes in regions exhibiting a spreading interaction pattern in the primary analysis.

Brain patch/cluster sizes and clinical-cognitive changes. We analyzed cortical patches and subcortical-cortical clusters that exhibited significant changes pre- to post-treatment, as identified by the spreading interaction analysis. Specifically, we investigated the associations between significant changes in patch/cluster sizes and changes in clinical-cognitive measures within the treatment group using linear regression. For each significant patch and cluster, we constructed a linear regression model for each of the eight clinical-cognitive measures, with patch or cluster size as the predictor. Age, gender, and the baseline score of the clinical-cognitive measure of interest were included as covariates in the models. Due to missing data for the PRT, participants with incomplete data were excluded from specific analyses (see Table 1). Given the exploratory nature of this analysis, both uncorrected and FDR-corrected *p*-values (*q*-values) from the models were reported.

RESULTS

Brain changes

Cortical patch sizes. In our examination of the cortical patch sizes, no significant patches were identified from the whole-network level analysis after correcting for multiple comparisons. In the ROI analysis, the right medial posterior prefrontal cortex (PFCmp) within the Control B network (i.e. component B in the frontoparietal control network as described in refs. [26, 30]; Fig. 2A) demonstrated a statistically significant Group x Session interaction effect ($b = -3.55$, SE $= 1.67$, $p = 0.037$; Fig. 2B). Spreading interaction test confirmed that the pre- to post-treatment size decrease in the right PFCmp was specific to the group that received the KOR antagonist ($p = 0.013$, FDR-corrected across hemisphere $p = 0.026$, $q < 0.05$; Fig. 2C).

Subcortical-cortical cluster sizes. In our analysis of the subcortical-cortical clusters, no significant clusters were

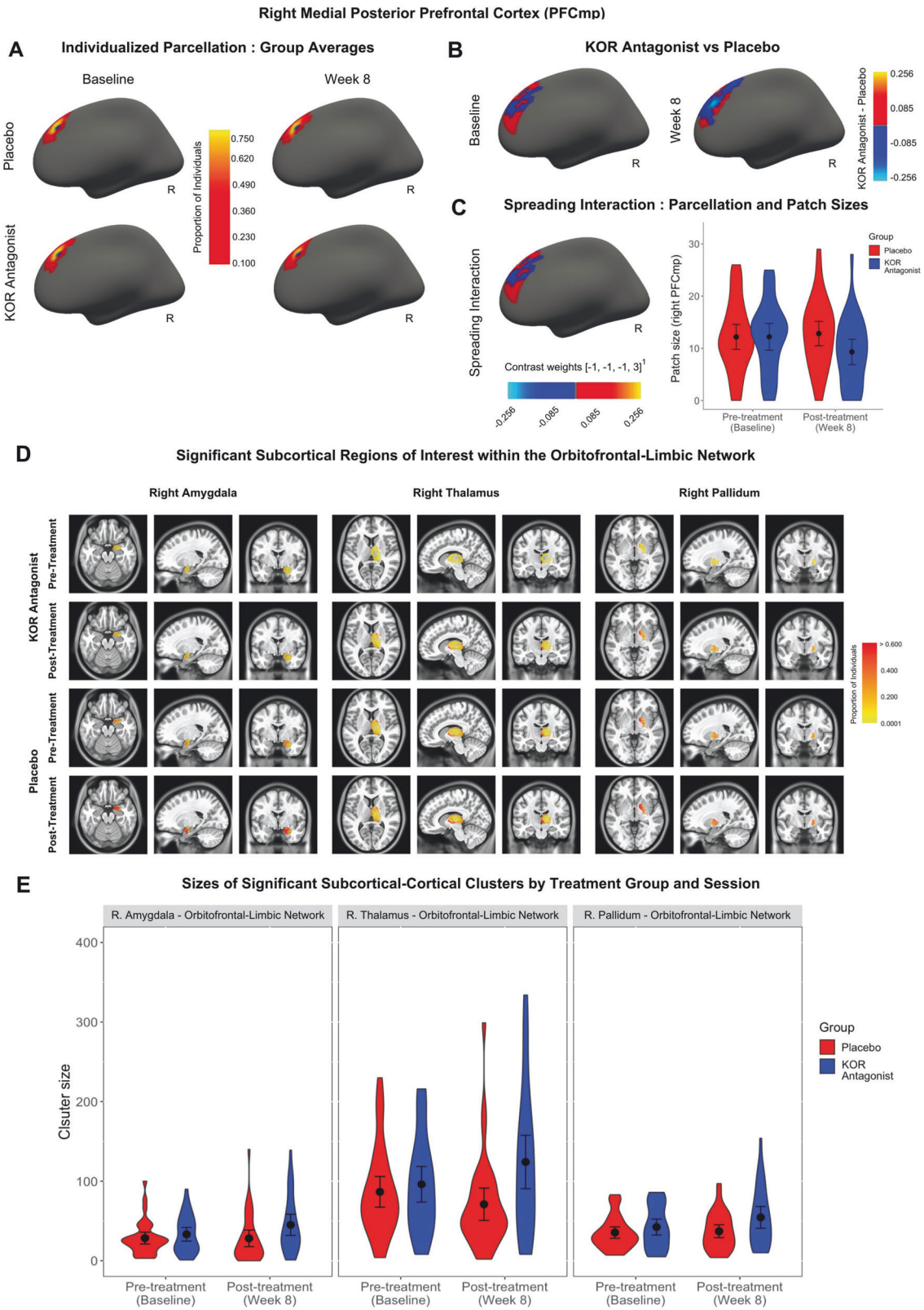

identified from the whole-network level analysis after correcting for multiple comparisons. In the ROI analysis, three subcortical clusters within the orbitofrontal-limbic network were significant after FDR correction ($q < 0.05$): the right pallidum ($t = 2.99$, $p = 0.0033$), right amygdala ($t = 2.72$, $p = 0.0076$), and right thalamus ($t = 3.04$, $p = 0.0029$) (see Fig. 2D). These results revealed significant size increases in three subcortical structures within the orbitofrontal-limbic system [21, 32] following the KOR antagonist treatment. The same pattern was not observed in the placebo group (see Fig. 2E).

Fig. 2 Significant cortical patch of interest: right medial posterior prefrontal cortex (PFCmp) patch within the frontoparietal control network and significant subcortical-cortical clusters of interest. Panel **A** Individual-specific right PFCmp patches obtained from the individualized brain systems mapping approach, averaged by treatment group and session. Blue dot represents the center of mass, and the color bar shows the proportion of individuals showing overlap in the parcellation. Specifically, the proportion indicates how many individuals share similar PFCmp patches, with higher values corresponding to greater overlap; Panel **B** Differences in right PFCmp patches between the KOR antagonist and placebo groups at baseline (left) and week eight (right); Panel **C** (Left) Differences in right PFCmp patches between the KOR antagonist post-treatment session and other sessions. (Right) Violin plot showing right PFCmp patch sizes by treatment group and session, and illustrating significant spreading interaction, where the average right PFCmp patch size of the antagonist post-treatment session is smaller than the other sessions. [1] Contrast weights [−1, −1, −1, 3]: The weights used to test for spreading interaction [−1 (pre-treatment, placebo), −1 (pre-treatment, KOR antagonist), −1 (post-treatment, placebo), 3 (post-treatment, KOR antagonist)]. Panel **D** Individual-specific subcortical-cortical clusters obtained from the individualized brain systems mapping approach, by treatment group and session. Only the three subcortical regions in the orbitofrontal-limbic network displaying significant spreading interaction based on cluster size are shown. The color bar shows the proportion of individuals showing overlap in the parcellation, with higher values corresponding to greater overlap. Panel **E** Violin plots showing cluster sizes, by group and session, of subcortical-cortical clusters exhibiting significant spreading interaction.

Brain and clinical-cognitive changes

Right PFCmp patch size change and clinical-cognitive changes. Linear regression models revealed that the significant patch size decrease in the right PFCmp was not associated with any of the clinical and cognitive measures being investigated in the study.

Subcortical-cortical cluster size change and clinical-cognitive changes. None of the three subcortical-cortical clusters that showed a size increase after treatment was significantly linked to any clinical-cognitive changes after correcting for multiple comparisons. However, the size increase in the right amygdala within the orbitofrontal-limbic network showed a trend association with improvement in the cognitive and physical functioning scale ($b = -0.061$, SE = 0.031, $p = 0.0583$, $q = 0.233$; Fig. 3A, B) and PRT Task Reward Sensitivity ($b = 0.0045$, SE = 0.0022, $p = 0.0522$, $q = 0.233$; Fig. 3C, D).

DISCUSSION

This study is the first to examine post-KOR antagonist treatment brain changes in a transdiagnostic anhedonia sample using an individualized brain systems functional brain mapping approach. Our results revealed a significant decrease in the size of the right medial posterior prefrontal cortex within the frontoparietal control network (also commonly known as the central executive network) following KOR antagonist treatment. Additionally, we observed significant size increases in three subcortical clusters, 1) right pallidum, 2) right amygdala, and 3) right thalamus, within the orbitofrontal-limbic network. Statistical analyses of the clinical-cognitive measures showed that both the KOR antagonist group and the placebo group exhibited improvements in anhedonia and other clinical outcomes. However, unlike the full FAST-MAS cohort [15], the difference in SHAPS scores between the two groups at the end of the treatment period was not significant in this subsample of participants who completed both MRI scans. This suggests that although brain alterations were observed after eight weeks of KOR antagonist treatment compared to placebo, they may not be associated to the improvements seen in the clinical and cognitive outcomes. Indeed, findings from our exploratory analysis showed that changes in patch and cluster sizes were not significantly correlated with changes in clinical and cognitive measures for the KOR antagonist group after correcting for multiple comparisons. However, it is worth noting that size increase in the right amygdala within the orbitofrontal-limbic system demonstrated a borderline significant relationship with improvement in cognitive and physical functioning, as well as increased sensitivity to rewards in the PRT Task.

Despite the absence of a brain-clinical outcome relationship, this study provides valuable insights into the neurobiological effects of the KOR antagonist in a transdiagnostic sample of individuals exhibiting anhedonia. The prefrontal cortex, nucleus accumbens, caudate, putamen, pallidum, thalamus, amygdala and hippocampus have consistently been identified as key regions implicated in mood and anxiety disorders (for a review, see refs. [33–36]). For instance, previous brain-imaging studies of MDD have revealed alterations in gray matter, white matter, synaptic density, and neuronal activity within these areas. Circuitries involving these regions, including the prefrontal-subcortical circuit, prefrontal-hippocampal circuit, and frontothalamic circuit, have also been found to be impaired in MDD [36, 37]. As core components of the reward circuit, these regions play essential roles in processing reward-related information and responding to rewarding stimuli [38], which are foundational to understanding the mechanisms underlying anhedonia. Broadly speaking, the medial prefrontal cortex (mPFC) plays a critical role in evaluating rewards and guiding decision-making, the orbitofrontal cortex (OFC) encodes reward value and contributes to the subjective experience of pleasure, and the amygdala is integral to reward prediction, particularly in emotional contexts [11]. Rather than operating in isolation, however, the cortical and subcortical areas in the reward circuit form complex networks to mediate different aspects of reward processing, including reward liking (consummatory phase), reward wanting (appetitive/anticipatory phase), and reward learning [39, 40]. Alterations in these areas are linked to anhedonia and other reward-related deficits across various disorders [11]. Notably, multiple meta-analyses and systematic reviews [39, 41] have identified common frontostriatal abnormalities – specially, hypoactivation in the striatum and OFC, alongside hyperactivation in the medial prefrontal cortex – that underlie deficits across aspects of reward processing in MDD. The functionally and individually derived patches in the current study reflect the amount of brain areas devoted to specific functional networks, hence the decrease in functional units in the medial posterior prefrontal cortex and increase in functional units in the pallidum, thalamus, and amygdala may indicate a normalization of the brain activity pattern following KOR antagonist treatment.

Furthermore, our finding of the reduced right PFCmp aligns with previous research indicating functional cerebral asymmetry in MDD. There is a well-documented association with hypoactivity in the left and hyperactivity in the right frontal areas during task and rest [42, 43]. The right frontal area is implicated in the inhibition and suppression of urges, and an increase in right frontal activity has been linked to reduced craving for food in healthy individuals. Consequently, heightened activity in the PFCmp may be associated with an over-inhibition of natural hedonic instincts, potentially contributing to anhedonia [42]. While the current study did not directly investigate inter-hemispheric dynamics, the observed reduction in functional units in the right PFCmp raises the possibility of a normalization process. Future investigations could further explore this aspect by examining the balance between the left and right PFCmp patches pre- and post-treatment. Interestingly, the three identified subcortical-orbitofrontal clusters are also located within the right hemisphere. Nevertheless, it is important to acknowledge that functional asymmetry in subcortical areas is

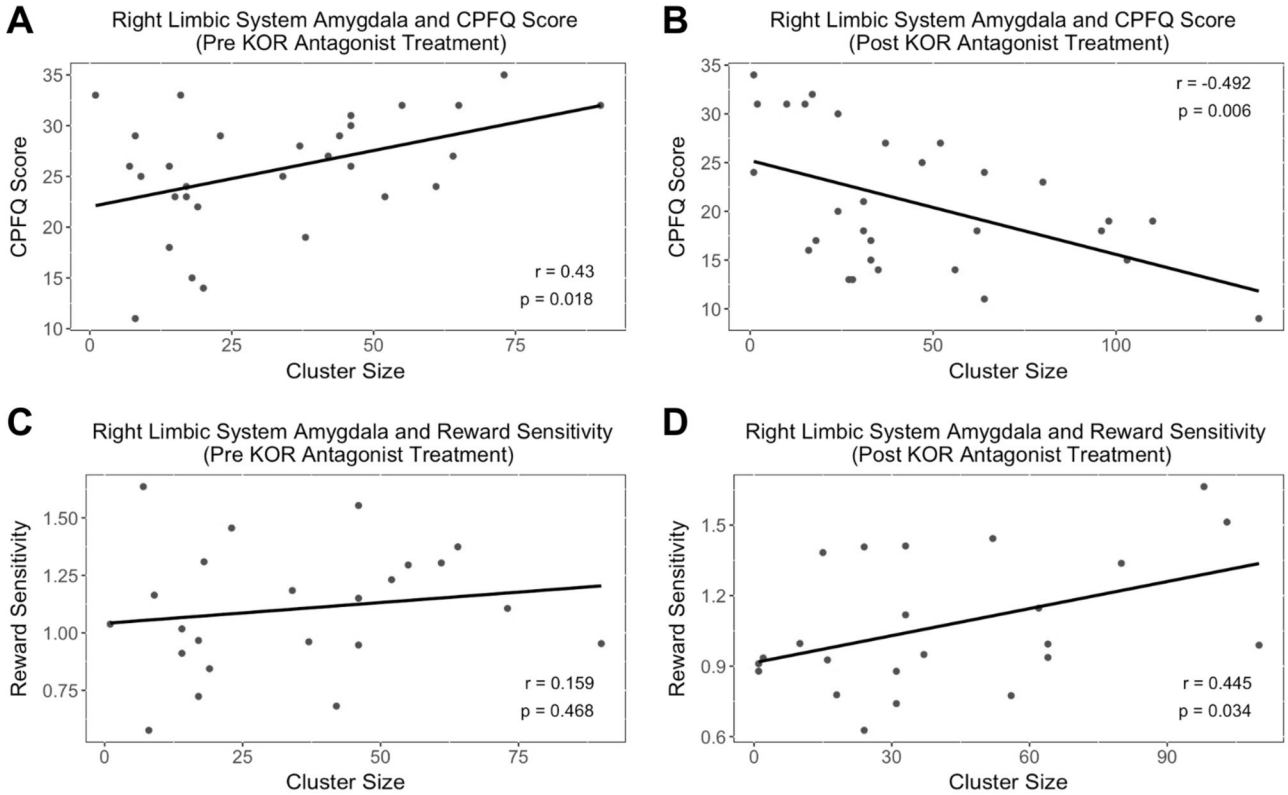

Fig. 3 Correlations between cluster sizes and cognitive functioning. Scatter plots of cluster sizes and cognitive measures where change in subcortical-cortical cluster sizes pre to post KOR antagonist treatment show a trend association with improvement in cognitive functioning. Panels **A**–**D** Correlations between cluster size of the right amygdala within the orbitofrontal-limbic system and (Panel **A** CPFQ score pre-treatment; Panel **B** CPFQ score post-treatment; Panel **C** reward sensitivity in the probabilistic reward task pre-treatment; Panel **D** reward sensitivity in the probabilistic reward task post-treatment). CPFQ Cognitive and Physical Functioning Questionnaire, higher scores indicate more severe cognitive dysfunction.

comparatively less explored in the existing literature. Structurally, Zuo et al. found abnormalities in structural asymmetry in patients with MDD in the nucleus accumbens, pallidum and thalamus [44]; however, a recent study which examined structural asymmetries in subcortical areas across a cohort of 2540 individuals with MDD and 4230 control subjects, reported no significant structural asymmetry in MDD [45]. These mixed findings underscore the complexity of asymmetrical patterns within the brain. Further exploration of functional asymmetries in subcortical areas may unveil additional insights into the intricate neural mechanisms underlying MDD and anhedonia.

Overall, the significant size decrease of the right medial posterior prefrontal cortex within the frontoparietal control network and increases of the right pallidum, amygdala, and thalamus within the orbitofrontal-limbic network following KOR antagonist treatment, may indicate a normalization process in the context of reward processing and anhedonia. However, the lack of noticeable behavioral changes—especially concerning anhedonia—and the absence of findings in other regions conventionally linked with reward processing, such as the nucleus accumbens and caudate, raise important questions about the specific nature of KOR antagonist treatment on the neurobiology of anhedonia. Further exploration of direct circuit measures, including a functional connectivity analysis utilizing individualized parcellation, may provide deeper insights into the mechanisms driving the observed neurobiological changes and their implications for anhedonia.

A limitation of this study is that the subsample of FAST-MAS study participants who completed both MRI scans and were therefore included in the current study is considerably smaller than the full cohort reported by Krystal et al. in 2020 [15]. In Krystal et al's study, there were 45 participants in the KOR antagonist group and 44 in the placebo group, whereas the current study only has 30 participants in the KOR antagonist group and 34 in the placebo group. This difference in sample size, combined with the heterogeneous nature of the study, reduces the statistical power of the current study. In addition, unlike the full cohort, the subsample did not exhibit a significant difference in improvements in anhedonia between the two groups, posing a challenge in examining and interpreting the relationships between brain changes and treatment efficacy. However, this study's application of an innovative neuroimaging analysis approach and focus on KOR antagonist treatment highlights the potential of this work to inform precision medicine approaches in transdiagnostic populations. Analyses related to associations between brain patch/cluster sizes and clinical-cognitive changes were exploratory, and future transdiagnostic studies would benefit from larger sample sizes to increase the robustness and interpretability of their results.

DATA AVAILABILITY

Study data are available through the NIH/NIMH data archive and are accessible by emailing NDAHelp@mail.nih.gov.

REFERENCES

1. American Psychiatric Association, D. S. M. T. F., American Psychiatric Association. Diagnostic and statistical manual of mental disorders: DSM-5. 5, Washington, DC: American psychiatric association; 2013.
2. Whitton, AE, Diego A. P. "Anhedonia in depression and bipolar disorder." In *Anhedonia: Preclinical, Translational, and Clinical Integration*, pp. 111-27. Cham: Springer International Publishing, (2022).

3. Serretti A. Anhedonia and depressive disorders. Clin Psychopharmacol Neurosci. 2023;21:401.
4. Pizzagalli DA, Smoski M, Ang YS, Whitton AE, Sanacora G, Mathew SJ, et al. Selective kappa-opioid antagonism ameliorates anhedonic behavior: evidence from the Fast-fail Trial in Mood and Anxiety Spectrum Disorders (FAST-MAS). Neuropsychopharmacology. 2020;45:1656–63.
5. Whitton AE, Kumar P, Treadway MT, Rutherford AV, Ironside ML, Foti D, et al. Distinct profiles of anhedonia and reward processing and their prospective associations with quality of life among individuals with mood disorders. Mol Psychiatry. 2023;28:5272–81.
6. Vinckier F, Gourion D, Mouchabac SJEP. Anhedonia predicts poor psychosocial functioning: results from a large cohort of patients treated for major depressive disorder by general practitioners. Eur Psychiatry. 2017;44:1–8.
7. Grahek I, Shenhav A, Musslick S, Krebs RM, Koster EHW. Anhedonia, but not irritability, is associated with illness severity outcomes in adolescent major depression. J Child Adolesc Psychopharmacol. 2015;25:194–200.
8. Dimick MK, Hird MA, Fiksenbaum LM, Mitchell RHB, Goldstein BI. Severe anhedonia among adolescents with bipolar disorder is common and associated with increased psychiatric symptom burden. J Psychiatr Res. 2021;134:200–7.
9. Schaub AC, Kirschner M, Schweinfurth N, Mählmann L, Kettelhack C, Engeli EE, et al. Neural mapping of anhedonia across psychiatric diagnoses: a transdiagnostic neuroimaging analysis. NeuroImage: Clin. 2021;32:102825.
10. Gorwood P. Neurobiological mechanisms of anhedonia. Dialogues Clin Neurosci. 2008;10:291–9.
11. Der-Avakian A, Markou A. The neurobiology of anhedonia and other reward-related deficits. Trends Neurosci. 2012;35:68–77.
12. Nagy GA, Cernasov P, Pisoni A, Walsh E, Dichter GS, Smoski MJ. Reward network modulation as a mechanism of change in behavioral activation. Behav Modif. 2020;44:186–213.
13. Cuthbert BN. The RDoC framework: facilitating transition from ICD/DSM to dimensional approaches that integrate neuroscience and psychopathology. World psychiatry. 2014;13:28–35.
14. Guineau MG, Ikani N, Rinck M, Collard RM, van Eijndhoven P, Tendolkar I, et al. Anhedonia as a transdiagnostic symptom across psychological disorders: a network approach. Psychological Med. 2023;53:3908–19.
15. Krystal AD, Pizzagalli DA, Smoski M, Mathew SJ, Nurnberger J Jr, Lisanby SH, et al. A randomized proof-of-mechanism trial applying the 'fast-fail'approach to evaluating κ-opioid antagonism as a treatment for anhedonia. Nat Med. 2020;26:760–8.
16. Carlezon WA Jr, Krystal AD. Kappa-opioid antagonists for psychiatric disorders: from bench to clinical trials. Depression anxiety. 2016;33:895–906.
17. Pizzagalli DA. Toward a better understanding of the mechanisms and pathophysiology of anhedonia: are we ready for translation? Am J Psychiatry. 2022;179:458–69.
18. Wu H, Mata J, Furman DJ, Whitmer AJ, Gotlib IH, Thompson RJ. Anticipatory and consummatory pleasure and displeasure in major depressive disorder: an experience sampling study. J Abnorm Psychol. 2017;126:149.
19. Wang D, Buckner RL, Fox MD, Holt DJ, Holmes AJ, Stoecklein S, et al. Parcellating cortical functional networks in individuals. Nat Neurosci. 2015;18:1853–60.
20. Li M, Wang D, Ren J, Langs G, Stoecklein S, Brennan BP, et al. Performing group-level functional image analyses based on homologous functional regions mapped in individuals. PLoS Biol. 2019;17:e2007032.
21. Greene DJ, Laumann TO, Dubis JW, Ihnen SK, Neta M, Power JD, et al. Developmental changes in the organization of functional connections between the basal ganglia and cerebral cortex. J Neurosci. 2014;34:5842–54.
22. Kong R, Li J, Orban C, Sabuncu MR, Liu H, Schaefer A, et al. Spatial topography of individual-specific cortical networks predicts human cognition, personality, and emotion. Cereb Cortex. 2019;29:2533–51.
23. Kong R, Yang Q, Gordon E, Xue A, Yan X, Orban C, et al. Individual-specific areal-level parcellations improve functional connectivity prediction of behavior. Cereb Cortex. 2021;31:4477–500.
24. Trivedi MH, McGrath PJ, Fava M, Parsey RV, Kurian BT, Phillips ML, et al. "Establishing moderators and biosignatures of antidepressant response in clinical care (EMBARC): rationale and design. J Psychiatr Res. 2016;78:11–23.
25. Sacchet MD, Keshava P, Walsh SW, Potash RM, Li M, Liu H, et al. Individualized functional brain system topologies and major depression: relationships among patch sizes and clinical profiles and behavior. Biol Psychiatry Cogn Neurosci Neuroimaging. 2024;9:616–25.
26. Yeo BT, Krienen FM, Sepulcre J, Sabuncu MR, Lashkari D, Hollinshead M, et al. "The organization of the human cerebral cortex estimated by intrinsic functional connectivity. J Neurophysiol. 2011;106:1125–65.
27. Zhang D, Snyder AZ, Fox MD, Sansbury MW, Shimony JS, Raichle ME. Intrinsic functional relations between human cerebral cortex and thalamus. J Neurophysiol. 2008;100:1740–8.
28. Creswell JD, Taren AA, Lindsay EK, Greco CM, Gianaros PJ, Fairgrieve A, et al. Alterations in resting-state functional connectivity link mindfulness meditation with reduced interleukin-6: a randomized controlled trial. Biol psychiatry. 2016;80:53–61.
29. Lifshitz M, Sacchet MD, Huntenburg JM, Thiery T, Fan Y, Gärtner M, et al. Mindfulness-based therapy regulates brain connectivity in major depression. Psychother Psychosom. 2019;88:375–7.
30. Baker JT, Holmes AJ, Masters GA, Yeo BT, Krienen F, Buckner RL, et al. Disruption of cortical association networks in schizophrenia and psychotic bipolar disorder. JAMA Psychiatry. 2014;71:109–18.
31. Benjamini Y, Hochberg Y. Controlling the false discovery rate: a practical and powerful approach to multiple testing. J R Stat Soc Ser B. 1995;57:289–300.
32. Kong R, Li J, Orban C, Sabuncu MR, Liu H, Schaefer A, et al. Corrigendum to: spatial topography of individual-specific cortical networks predicts human cognition, personality and emotion. Cereb Cortex. 2021;31:3974.
33. Price JL, Drevets WC. Neurocircuitry of mood disorders. Neuropsychopharmacology. 2010;35:192–216.
34. Russo SJ, Nestler EJ. The brain reward circuitry in mood disorders. Nat Rev Neurosci. 2013;14:609–25.
35. Martin EI, Ressler KJ, Binder E, Nemeroff CB. The neurobiology of anxiety disorders: brain imaging, genetics, and psychoneuroendocrinology. Psychiatr Clin. 2009;32:549–75.
36. Zhang FF, Peng W, Sweeney JA, Jia ZY, Gong QY. Brain structure alterations in depression: psychoradiological evidence. CNS Neurosci Therapeutics. 2018;24:994–1003.
37. Zhang FF, Peng W, Sweeney JA, Jia ZY, Gong QY. Lower synaptic density is associated with depression severity and network alterations. Nat Commun. 2019;10:1529.
38. Haber SN, Knutson B. The reward circuit: linking primate anatomy and human imaging. Neuropsychopharmacology. 2010;35:4–26.
39. Borsini A, Wallis ASJ, Zunszain P, Pariante CM, Kempton MJ. Characterizing anhedonia: a systematic review of neuroimaging across the subtypes of reward processing deficits in depression. Cogn Affect Behav Neurosci. 2020;20:816–41.
40. Husain M, Roiser JP. Neuroscience of apathy and anhedonia: a transdiagnostic approach. Nat Rev Neurosci. 2018;19:470–84.
41. Zhang WN, Chang SH, Guo LY, Zhang KL, Wang J. The neural correlates of reward-related processing in major depressive disorder: a meta-analysis of functional magnetic resonance imaging studies. J Affect Disord. 2013;151:531–9.
42. Hecht D. Depression and the hyperactive right-hemisphere. Neurosci Res. 2010;68:77–87.
43. Kustubayeva A, Kamzanova A, Kudaibergenova S, Pivkina V, Matthews G. Major depression and brain asymmetry in a decision-making task with negative and positive feedback. Symmetry. 2020;12:2118.
44. Zuo Z, Ran S, Wang Y, Li C, Han Q, Tang Q, et al. Asymmetry in cortical thickness and subcortical volume in treatment-naïve major depressive disorder. NeuroImage Clin. 2019;21:101614.
45. De Kovel CGF, Aftanas L, Aleman A, Alexander-Bloch AF, Baune BT, Brack I, et al. No alterations of brain structural asymmetry in major depressive disorder: an ENIGMA consortium analysis. Am J Psychiatry. 2019;176:1039.

AUTHOR CONTRIBUTIONS

Hoki Fung: Conceptualization, Analysis, Visualization, Writing - original draft, Writing - review & editing. Andrew Krystal: Conceptualization, Writing - review & editing. Diego A. Pizzagalli: Conceptualization, Writing - review & editing. Ruby M. Potash: Writing - review & editing. Matthew D. Sacchet: Conceptualization, Writing - original draft, Writing – review.

FUNDING

This research is supported by the National Institute of Mental Health (Project Number R01MH125850) and Brain and Behavior Research Foundation (Grant Number 28972), Rappaport Foundation, The Ride for Mental Health, and Gatto Foundation.

COMPETING INTERESTS

Over the past 3 years, DAP has received consulting fees from Boehringer Ingelheim, Compass Pathways, Engrail Therapeutics, Karla Therapeutics, Neumora Therapeutics, Neurocrine Biosciences, Neuroscience Software, Otsuka, Sage Therapeutics, Sama Therapeutics, Sunovion Therapeutics, and Takeda; he has received honoraria from the American Psychological Association, Psychonomic Society and Springer (for editorial work) as well as Alkermes; he has received research funding from the Brain

and Behavior Research Foundation, Dana Foundation, Wellcome Leap, Millennium Pharmaceuticals, and NIMH; he has received stock options from Compass Pathways, Engrail Therapeutics, Neumora Therapeutics, and Neuroscience Software. No funding from these entities was used to support the current work, and all views expressed are solely those of the authors. All other authors have no conflicts of interest or relevant disclosures.

ADDITIONAL INFORMATION

Supplementary information The online version contains supplementary material available at https://doi.org/10.1038/s41386-025-02125-z.

Correspondence and requests for materials should be addressed to Matthew D. Sacchet.